

UDC 678.742.3:678.742.2

Sardorbek Otajonov^a, *Khamdam Akbarov*^a, *Nuritdin Kattaev*^a, *Elyor Berdimurodov*^a,
Abdugafur Mamadalimov^b, *Shokhzod Norbekov*^b, *Yong Ill-Lee*^c

SYNTHESIS, ELECTROPHYSICAL, AND OPTICAL PROPERTIES OF CONDUCTIVE POLYMERS BASED ON POLY(1-N-VINYLMIDAZOLE)

^a Department of Chemistry, National University of Uzbekistan, Tashkent, Uzbekistan

^b Department of Physics, National University of Uzbekistan, Tashkent, Uzbekistan

^c Department of Chemistry, Changwon National University, Changwon, Republic of Korea

Poly(1-N-vinylimidazole) (PVI_m) was obtained by the radical polymerization of 1-N-vinylimidazole in a benzene solution under an inert atmosphere at a temperature of 60°C. Its hydrophilic derivative was synthesized by chemical modification of PVI_m with 3-bromopropylamine hydrobromide. The structure of the synthesized polymers was studied by IR spectroscopy. The electrophysical and optical properties of PVI_m and its derivatives were studied. The temperature dependence of electrical conductivity, voltammetric behavior, photoconductivity kinetics, and optical band gap values of these polymer materials were determined. This work was carried out in the 300–360 K temperature range and in the 0–100 V voltage range. It was confirmed that electrical conductivity in all samples obeyed Ohm's law.

Keywords: 1-N-vinylimidazole, radical polymerization, chemical modification, electrical conductivity, photoconductivity, voltammetric characteristics.

DOI: 10.32434/0321-4095-2025-161-4-31-40

Introduction

In the past few decades, electrically conductive polymers (CPs) have attracted significant attention due to their strong potential as an alternative to their inorganic counterparts in fundamental and applied research. In the late 1970s, many scientists considered CPs (or «synthetic metals») to be difficult to treat and insoluble in water. Since the discovery of polyacetylene in 1977 by Hideki Shirakawa, Alan MacDiarmid, and Alan Heeger, various important CPs, such as polypyrrole (PPy), polyaniline (PANI), polythiophene (PT), poly(3,4 ethylenedioxythiophene) (PEDOT), trans polyacetylene, and poly(p phenylvinylene) (PPV), have been continuously investigated [1].

More generally, CPs have alternating single (σ) and double (π) bonds, leading to π -conjugated, which gives CPs unique optical, electrochemical, electrical, and electronic properties. It is known that the

parameters that most influence the physical properties of CPs are the length of their conjugation, the degree of crystallinity, and intra-chain and inter-chain interactions. CPs provide advantages such as chemical diversity, low density, flexibility, and corrosion resistance, easily controllable shape and morphology, as well as adjustable permeability compared to existing inorganic analogues [2,3]. However, the intrinsic properties of CPs still lag behind those of their metallic and inorganic semiconductor counterparts due to inherent limitations in solubility, electrical conductivity, and long term stability. Therefore, CPs are often modified or hybridized with other materials to overcome these shortcomings. A smart combination of CPs with other materials can lead to materials with attractive features and new application opportunities in different areas, from electronics to energy devices. Researchers in this field reported various

© Sardorbek Otajonov, Khamdam Akbarov, Nuritdin Kattaev, Elyor Berdimurodov, Abdugafur Mamadalimov, Shokhzod Norbekov, Yong Ill-Lee, 2025



This article is an open access article distributed under the terms and conditions of the Creative Commons Attribution (CC BY) license (<https://creativecommons.org/licenses/by/4.0/>).

Synthesis, electrophysical, and optical properties of conductive polymers based on poly(1-N-vinylimidazole)

strategies for preparing hybrids with CP-based compositions, new structures, and improved features.

CP nanocomposites containing carbon nanomaterials, such as graphene, carbon nanotubes, and carbon black, have been developed [4–7]. These carbon nanomaterials improve the systematic arrangement of CP chains and facilitate the delocalization of charge carriers, which lead to an increase in conductivity. Conductivity values ranging from insulating to metallic regimes were achieved [2,3,8]. Successful preparation of CPs composites with high mechanical stability, flexibility, and electrical conductivity proved that CPs can serve as the main material components in LEDs [9,10], transistors [11,12], electrochromic devices [13,14], actuators [15], electrochemical capacitors, photovoltaic elements, and sensors. Achieving precise control over the electrical and electrochemical properties of CPs is crucial for progress in these applications. Accordingly, this review focuses on the latest developments in CP property modulation and summarizes recent experimental findings. This review also summarizes recent research trends in the application of CPs.

Therefore, expanding the scope of research allows us to reveal the general laws of the electrophysical properties of fibrous polymers, the mechanisms of electronic processes occurring in polymers, and the development of discrete electronic components. We selected poly(1 N vinylimidazole) and its derivatives as the research subject. The mechanism of electrical conductivity of a polymer is mainly characterized by conductivity parameters such as the density and mobility of charge carriers. The impact of dopants on polymer conductivity is significant. Chemical, photochemical, or electrochemical doping introduces external charge carriers into organic semiconductors. Depending on their chemical structure and reaction with the macromolecular matrix, additives reduce the resistance of polymers to different degrees.

It is known that most of the current conducting polymers, such as doped polypyrrole, polythiophene, and polyaniline, and their derivatives are characterized

by insolubility in solvents, instability in air, and other disadvantages. The presence of heteroatoms (e.g., N and S) in the polymer backbone enhances their electrical conductivity. The electronegativity and inductive effects of substituents influence polymer electronic properties by modulating donor–acceptor behavior. In principle, with appropriate substituents and dopants, even non conjugated polymers like poly(1 N vinylimidazole) can exhibit significant charge transfer between the dopant and polymer matrix.

Materials and methods

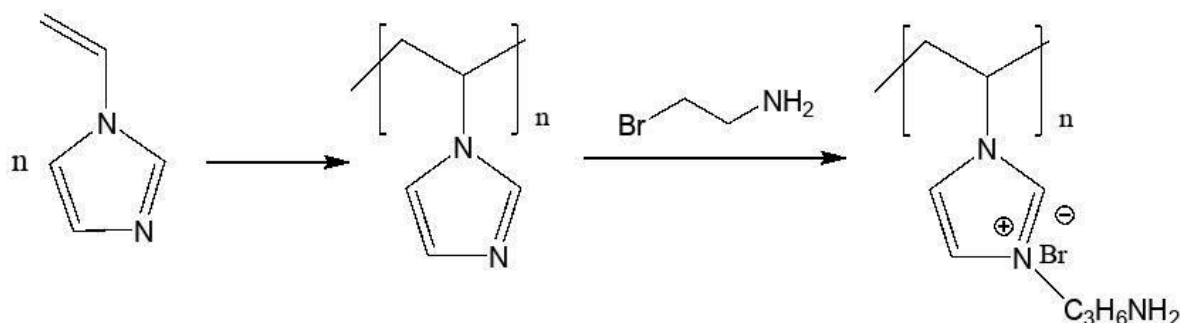
In this study, we used 1-vinylimidazole (Alfa Aesar), and 3-bromopropylamine hydrobromide (98%, Alfa Aesar).

Synthesis of novel PVI_m-Pro-NH₂

Poly(1-vinylimidazole) (PVI_m) was prepared according to the previously reported method with some modifications (Scheme 1). 9.624 mL (0.106 mol) of 1-vinylimidazole monomer and 100 mg (0.61 mmol) of AIBN were fully dissolved in 96 mL of benzene in a 250 mL three-necked round-bottom flask with mild stirring and heating. The mixed solution was heated under reflux at 60°C for 24 h under a nitrogen atmosphere. After the polymerization, the product was precipitated by the addition of acetone and then washed three times with acetone and hexane, respectively. The obtained PVI_m (faint yellow powder) was dried in a vacuum oven at 40°C for 48 h.

Then, 1 g (10 mmol; based on the monomer) of PVI_m and 3.07 g (30 mmol) of 3-bromopropylamine hydrobromide at a 1:1.5 molar ratio were added to 50 mL of ethanol, and the mixture was sonicated to ensure complete dissolution. The reaction mixture was heated at 60°C for 48 hours with constant stirring under reflux and a nitrogen atmosphere. The precipitated PVI_m-Pro-NH₂ was washed with hexane and dried in a vacuum oven at 40°C for 48 h.

A standard method was used to measure the current–voltage (I–V) characteristics at T=300 K. The experiment was performed both in the dark and under ultraviolet (UV) light ($\lambda=254$ nm). A Keithley



Scheme 1. The synthetic route of poly[VIImAm]Br

2461 SourceMeter with nanoampere sensitivity was used to obtain high-quality results. The measurement error in the I–V characteristics was approximately 2–4%. To determine the temperature dependence of the electrical conductivity of the polymers, a thermostat designed to maintain the temperature in a range from –250 to 1200°C was used to control the heater. The accuracy of the device was about 0.200°C. A copper–constantan (type T) thermocouple was used to monitor the temperature. The DC voltage applied to the sample was 0–100 V. Since the samples mainly have high resistance, the experiment was carried out using a UI-2 type electrometer connected to a computer for data acquisition. The sample was placed at the focal point of the lens and uniformly illuminated across the entire surface. A mercury lamp with a spectral energy of 5 eV was used to study photoconductivity kinetics.

Results and discussion

Characterization of PVIm-Pro-NH₂

The properties of synthesized PVIm-Pro-NH₂ were characterized by FT-IR and GPC. As shown in Fig. 1, the FT-IR spectra of PVIm (top) and PVIm-ET-NH₂ (bottom) demonstrate that the polymerization of PVIm and its alkylation with Pro-NH₂ were successful. Both spectra contain stretching vibrations corresponding to imidazole ring modes. For PVIm, the peaks are located at 1500.34, 1418.38, 1286.28, and 1230.36 cm⁻¹. For PVIm-Pro-NH₂, the corresponding peaks are found at 1496.49, 1418.38, 1285.32, and 1229.39 cm⁻¹. The bands at 1110.79 and 1088.61 cm⁻¹ can be assigned to the stretching vibrations of azole C–H groups. Bending vibrations of heterocyclic rings appear at 918.91, 826.34, and 747.28 cm⁻¹ for PVIm, and at 921.80, 830.20, and 749.20 cm⁻¹ for PVIm-Pro-NH₂. The characteristic N–H bending and C–N stretching peaks at 1568.80 and 1160.93 cm⁻¹ (PVIm-Pro-NH₂) confirm successful conversion of PVIm to PVIm-Pro-NH₂ via alkylation.

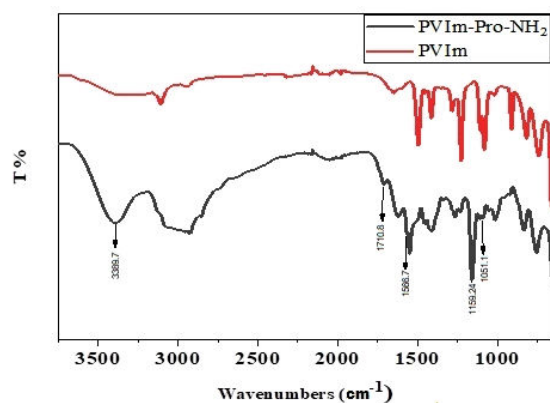


Fig. 1. FT-IR spectra of PVIm and PVIm-Pro-NH₂

To determine the molecular weight of PVIm-Pro-NH₂, GPC analysis was conducted in a 0.02 N sodium nitrate aqueous eluent. Table 1 shows the weight-average molecular weight (Mw), number-average molecular weight (Mn), and polydispersity index (PDI) of PVIm-Pro-NH₂. Mw, Mn, and PDI values are 407,878, 346,787, and 1.18, respectively.

In the images at 100× magnification (Fig. 2a and 2c), it was found that PVIm exhibits a granular morphology, while PVIm-Pro-NH₂ displays a fibrous structure. Highly agglomerated particles are clearly visible in the photomicrograph of PVIm at 2000× magnification (Fig. 2b). Pores are clearly observed on the surface of the particles. The fibrous morphology of PVIm-Pro-NH₂ is retained even at 2000× magnification (Fig. 2d). Energy-dispersive X-ray spectroscopy (EDS) was used to analyze the elemental composition. According to EDS analysis, the sample of PVIm contains 52.95% carbon and 47.05% nitrogen.

Table 1
GPC data for PVIm-Pro-NH₂. Eluent: 0.02 N sodium nitrate (aqueous solution)

Weight-average molecular weight (Mw)	Number-average molecular weight (Mn)	Polydispersity index (PDI)
407,878	346,787	1.18

Figure 3 presents the EDS analysis of PVIm-Pro-NH₂. The EDS spectrum shows that the modified polymer contains 47.48% carbon, 32.52% nitrogen, and 19.90% bromine.

Background on non-isothermal decomposition kinetics

Kinetic analysis of a thermal decomposition process typically yields three key parameters: activation energy (E_a), the pre-exponential factor (A), and the reaction model function $f(\alpha)$, where α represents the extent of conversion. The reaction mechanism model can take various forms depending on nucleation and growth, phase boundary reactions, diffusion, or chemical reaction control.

The general kinetic equation for non-isothermal decomposition is given by:

$$\frac{d\alpha}{dt} = k(T)f(\alpha), \quad (1)$$

where k is the rate constant; and α is the extent of conversion, defined as follows:

$$\alpha = \frac{m_i - m_t}{m_i - m_f}, \quad (2)$$

where m_i is the initial mass of the sample; m_t is its

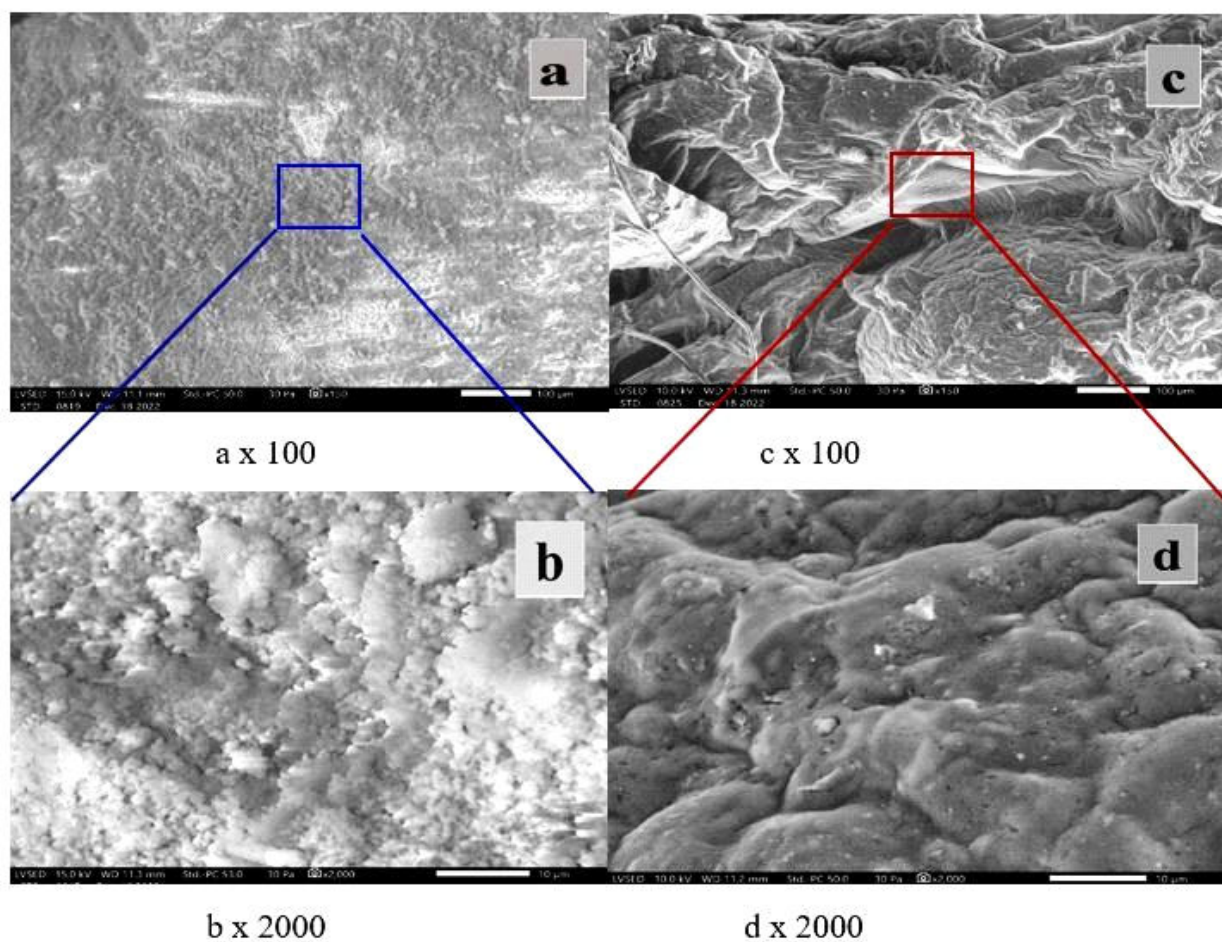


Fig. 2. Structural morphology of PVIm (a, b) and PVIm-Pro-NH₂(c, d)

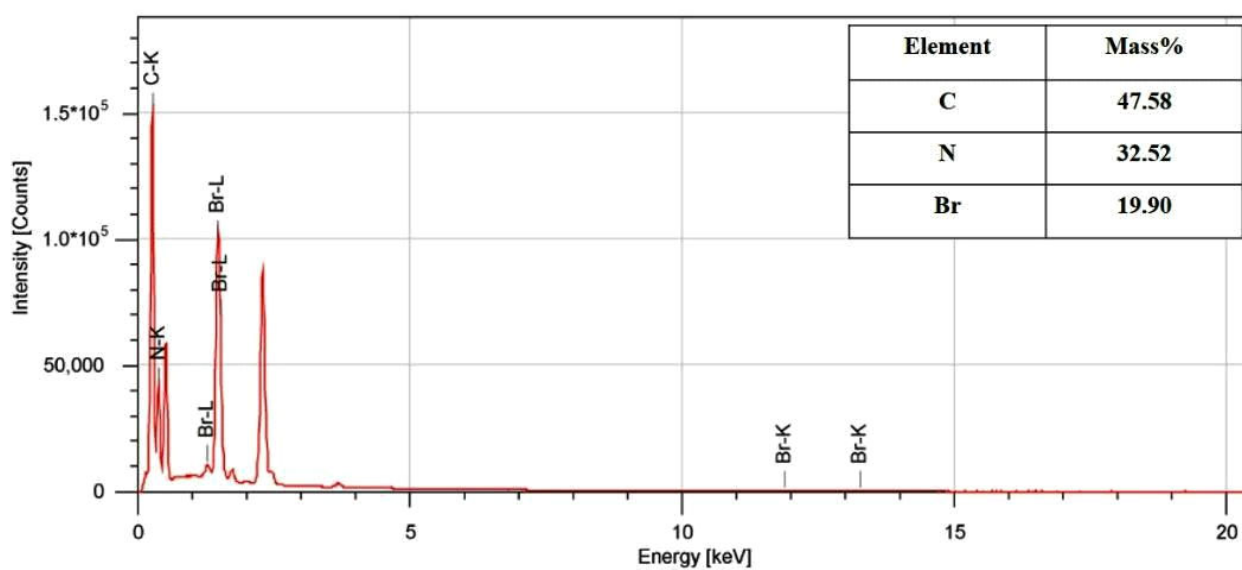


Fig. 3. EDS spectrum of PVIm-Pro-NH₂

mass at time t ; and m_f is the residual mass remaining after the reaction.

Integration of Eq. (1) gives the integral rate law:

$$g(\alpha) = kt. \quad (3)$$

The rate constant, k , is generally given by the Arrhenius equation:

$$k = A \exp\left(-\frac{E_a}{RT}\right). \quad (4)$$

where E_a is the activation energy; R is the gas constant; and T is the absolute temperature.

The combination of Eqs. (1) and (4) gives the following relationship:

$$\frac{d\alpha}{dt} = A \exp\left(-\frac{E_a}{RT}\right) f(\alpha). \quad (5)$$

For a dynamic thermogravimetric (TG) process, introducing the heating rate, $\beta = dT/dt$, into Eq. (5) yields the following equation:

$$\frac{d\alpha}{dt} = \frac{A}{\beta} \exp\left(-\frac{E_a}{RT}\right) f(\alpha). \quad (6)$$

Decomposition kinetics

TGA/DTA is a widely used technique to evaluate the thermal stability of inorganic or organic materials such as polyvinylimidazole. A typical TGA/DTA dynamic heating curve under Ar atmosphere to optimize the weight loss profile of a polyvinylimidazole sample can be observed in the diagram as a function of temperature (dynamic heating). The TGA plots indicated that PVIIm (polyvinylimidazole) exhibits the highest thermal-stability up to ca. 366.53°C with a weight loss of 60.996%, followed by PVIIm-Pro-NH₂ with weight loss of 71.095% at a temperature of 249.77°C. On the other hand, the PVIIm sample is thermally unstable and starts to decompose at above approximately 100°C in three steps (at approximately 100°C dehydration and at 339.52°C thermal decomposition), which may be due to its monolayer structure or distorted heptazine units. Moreover, a slow thermal deformation/decomposition for PVIIm and PVIIm-Pro-NH₂ materials followed by an abrupt sharp weight loss was observed, ending at 723°C and 722°C for PVIIm and PVIIm-Pro-NH₂, with total weight loss of about 95.8% and 100%, respectively. These changes were accompanied by sharp endothermic effects visible in the DTA curves (Fig 4).

The thermal deformation kinetic parameters (E_a and A) of the studied compounds were determined using the fraction a in the range $0.1 < a < 0.8$ obtained

from a thermoanalytical curve at a single heating rate (approximately 100°C/min). In this study, four calculation methods were employed to obtain the kinetic data: Coats and Redfern (Eq. (7)), Madhusudanan-Krishnan-Ninan (Eq. (8)), Wanjun et al. (Eq. (9)), and Tang et al. (Eq. (10)), as well as mechanism models.

$$\ln\left(\frac{g[\alpha]}{T^2}\right) = \ln\left[\frac{AR}{\beta E_a}\left(1 - \frac{2RT}{E_a}\right)\right] - \frac{E_a}{RT} \cong \ln\left(\frac{AR}{\beta E_a}\right) - \frac{E_a}{RT} \quad (7)$$

$$\ln\left(\frac{g[\alpha]}{T^2}\right) = \ln\left[\frac{AR}{\beta(1.0019882E + 1.87391198RT_p)}\right] - \frac{E_a}{RT} \quad (8)$$

$$\ln\left(\frac{g[\alpha]}{T^{1.894661}}\right) = \left[\ln\left[\frac{AE_a}{\beta R}\right] + 3.635041 - 1.894661 \ln E_a\right] - \frac{1.00145033E_a}{RT} \quad (9)$$

$$\ln\left(\frac{g[\alpha]}{T^{1.921503}}\right) = \left[\ln\left[\frac{AE_a}{\beta R}\right] + 3.772050 - 1.921503 \ln E_a\right] - \frac{0.120394E_a}{RT} \quad (10)$$

Plotting the left-hand sides of Eqs. (7)–(10) versus $1/T$ yields the values of A and E_a from the intercept and slope, respectively (Table 2). All mathematical calculations were performed in Excel

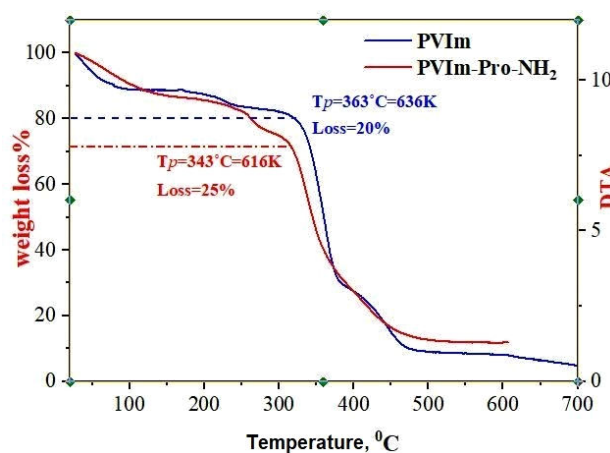


Fig. 4. Thermal analysis of PVIIm and PVIIm-Pro-NH₂

2016 to determine the pre-exponential factor and activation energy values. The values of the correlation coefficients are also presented in Table 2.

As can be seen from the results shown in Fig. 5, the current increases linearly with increasing voltage for both PVIIm and PVIIm-Pro-NH₂, under dark conditions and upon ultraviolet light saturation. This behavior can be described by Ohm's law.

It was observed that for PVIIm, when the voltage was increased from 0 to 100 V under dark conditions, the current increased sharply from 38 to 529 nA. In contrast, under ultraviolet light, the current increased from 84 to 813 nA over the same voltage range. A similar trend was observed for PVIIm-Pro-NH₂. Under dark conditions, increasing the voltage from 0 to 100 V resulted in a current increase from 0.12 to 0.68 mA. In contrast, when saturated with ultraviolet light, the current increased sharply from 1 to 5 mA over the same voltage range.

It is worth noting that in both cases (dark and UV-illuminated), the current in PVIIm-Pro-NH₂

(in mA) is approximately three orders of magnitude higher than that in PVIIm (in nA). The sharp increase in current under ultraviolet light compared to dark conditions can be attributed to the internal photoelectric effect.

To better understand the charge transport mechanism of PVIIm and PVIIm-Pro-NH₂, temperature-dependent current measurements were performed. The temperature dependence of the current at a constant voltage of $U=50$ V is shown in Fig. 6. To determine the activation energy, the Arrhenius plot was constructed using the function $\ln(I)$ versus $1000/T$, based on the Arrhenius equation.

It can be seen that the current at a given voltage increases with temperature and exhibits a linear trend in Arrhenius coordinates. A slight change in conductivity is observed at low temperatures, while a rapid increase is observed at higher temperatures. The temperature dependence of the current shown in Fig. 6 indicates a positive temperature coefficient of conductivity, confirming the semiconducting nature

Table 2

Kinetic parameters, activation energy (E_a) and pre-exponential factor (A), calculated using the Coats-Redfern (Eq. (7)), Madhusudanan-Krishnan-Ninan (Eq. (8)), Wanjun et al. (Eq. (9)), and Tang et al. (Eq. (10)) methods, based on correlation coefficients obtained from 35 decomposition mechanism models for polyvinylimidazole samples

Material	Parameter	Value			
		Eq. (7)	Eq. (8)	Eq. (9)	Eq. (10)
PVIIm	mechanism	F3/4	F3/4	G5	G6
	max R^2	0.9925	0.9925	0.9938	0.9938
	E_a , kJ/mol	126.547	126.547	340.521	380.336
	A	$3.1 \cdot 10^{10}$	$3.12 \cdot 10^{10}$	$1.74 \cdot 10^{27}$	$3.74 \cdot 10^{37}$
PVIIm-Pro-NH ₂	mechanism	D5	D5	F2	D5
	max R^2	0.9907	0.9907	0.9908	0.9908
	E_a , kJ/mol	146.816	146.816	85.153	122.271
	A	$1.031 \cdot 10^{11}$	$1.034 \cdot 10^{11}$	$5.6 \cdot 10^6$	$8 \cdot 10^{11}$

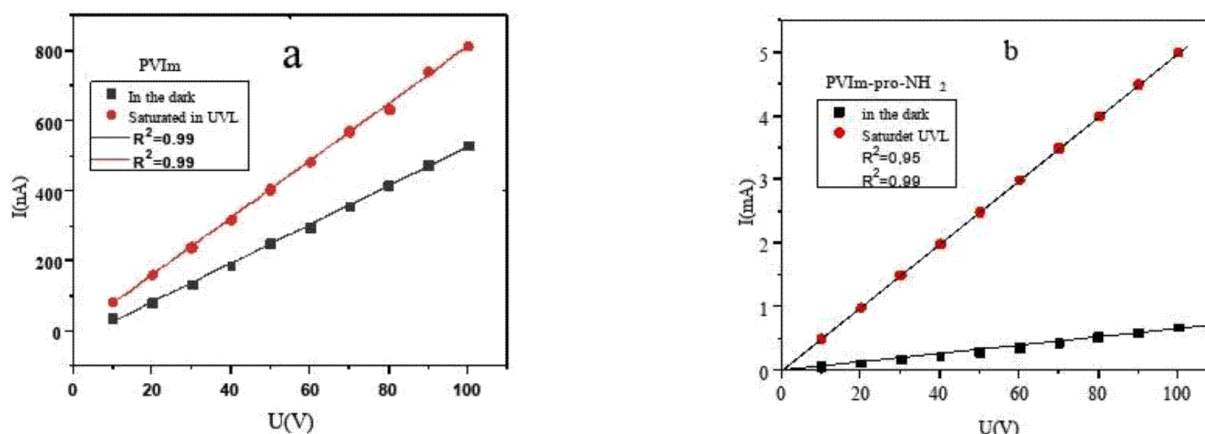


Fig. 5. Voltage-ampere characteristics of (a) PVIIm and (b) PVIIm-Pro-NH₂ polymers under ultraviolet light saturation (red) and in the dark (black) at $T=300$ K

of the materials.

The electrical conductivity of the samples increases with temperature, with activation energies of $E_{t1}=0.9$ eV for PVI_m and $E_{t1}=0.2$ eV for PVI_m-Pro-NH₂, respectively (Fig. 6). This temperature dependence follows an exponential law, indicating that the conductivity increases significantly with thermal activation energy. This suggests that the exponential relationship between electrical conductivity and temperature is influenced not only by internal transitions but also by the generation of charge carriers and other thermally activated processes.

The photoconductivity kinetics of the PVI_m and PVI_m-Pro-NH₂ samples was investigated (Fig. 7). The study shows an increase in photocurrent under UV illumination ($\lambda=254$ nm), followed by long-term relaxation of photoconductivity after the UV light is turned off. This indicates the manifestation of the

internal photoelectric effect. The steady-state value of photoconductivity is not reached instantly; instead, saturation occurs after a certain delay following light exposure of the semiconductor.

According to Fig. 7, after a certain period following the switching off of the light, the excess photoconductivity gradually disappears. The focus here is on the laws governing the increase and decay of photoconductivity depending on the illumination level. The change in the concentration of additional charge

carriers per unit time, $\frac{d(\Delta n)}{dt}$, is determined by the difference between the rates of generation and recombination of these carriers.

The decay curve of photoconductivity in Fig. 7 after the cessation of illumination reflects the recombination of the generated charge carriers, which proceeds according to a specific kinetic law. That is:

$$\Delta n = \Delta n_0 e^{-\frac{(t-t_0)}{\tau}}, \tag{11}$$

where t_0 is the time at which the illumination is switched off.

According to the same law, the photoconductivity of both PVI_m and PVI_m-Pro-NH₂ also exhibits an exponential decay:

$$\Delta \sigma_f = \Delta \sigma_{f0} e^{-\frac{(t-t_0)}{\tau}}. \tag{12}$$

The increase in photoconductivity in the sample after switching on the light pulse follows a law similar to that describing the photocurrent decay. That is:

$$\Delta \sigma_f = \Delta \sigma_{f0} \left(1 - e^{-\frac{t}{\tau}} \right). \tag{13}$$

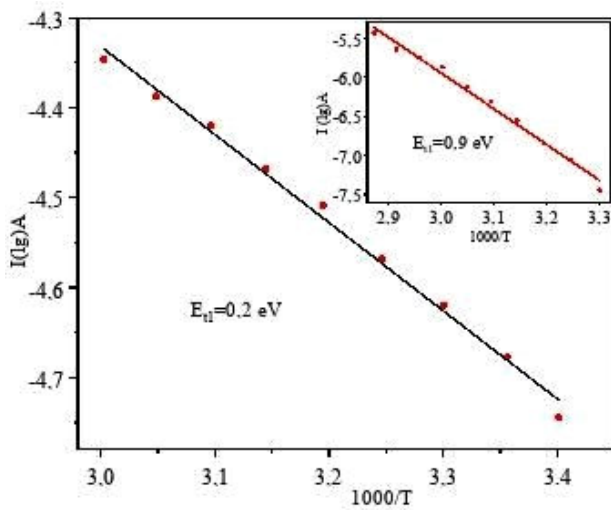


Fig. 6. Arrhenius plot of $\lg(I)$ versus $1000/T$ for PVI_m (inner curve) and PVI_m-Pro-NH₂ (outer curve)

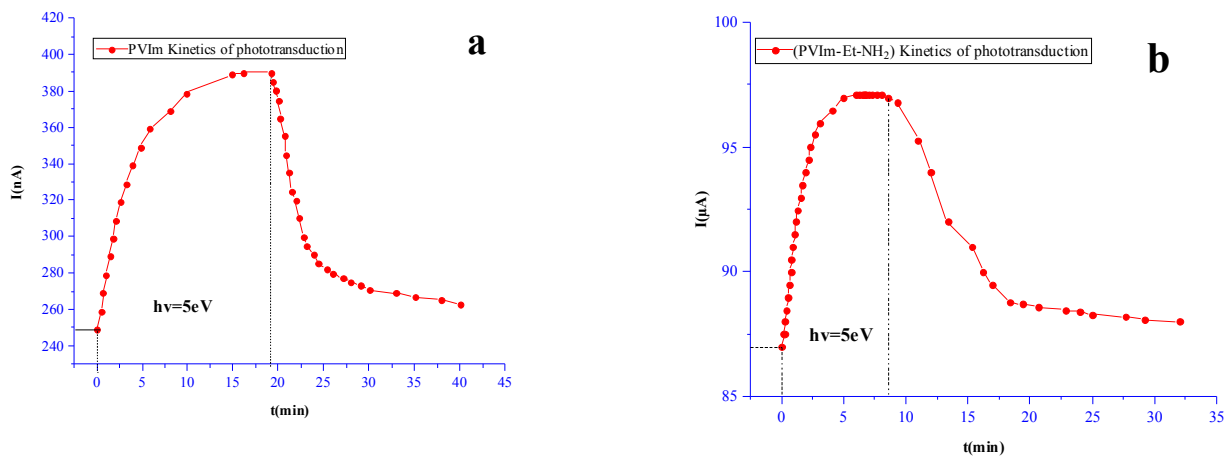


Fig. 7. Photoconductivity kinetics of (a) PVI_m and (b) PVI_m-Pro-NH₂ samples under specific optical transition at $T=300$ K

Here, t is the time elapsed from the onset of photoconduction to the point of saturation.

The electronic structures of the PVI_m and PVI_m-Et-NH₂ materials synthesized in this study were investigated using Diffuse Reflectance Electron Spectroscopy (DRES). The Kubelka-Munk function was applied to determine the optical band gaps of the polymers (Fig. 8a):

$$F(R)h\nu = A(h\nu - E_g)^2, \quad (14)$$

where F is the Kubelka-Munk function derived from the reflectance; E_g is the optical band gap energy of the semiconductor; h is Planck's constant; and ν is the frequency of the incident light.

The band gaps of the PVI_m and PVI_m-Et-NH₂ materials were determined graphically using Tauc plots (Fig. 8b). The band gaps were found to be 1.93 eV and 1.12 eV, respectively. These results indicate that the synthesized PVI_m and PVI_m-Pro-NH₂ materials possess semiconducting properties.

Conclusions

The synthesized poly(1-vinylimidazole) (PVI_m) and its hydrophilic derivative, PVI_m-Pro-NH₂, exhibit promising electrophysical and optical properties. The study confirms that both polymers obey Ohm's law, demonstrating linear current-voltage characteristics. Temperature-dependent conductivity measurements reveal semiconducting behavior with activation energies of 0.9 eV for PVI_m and 0.2 eV for PVI_m-Pro-NH₂. Photoconductivity experiments further indicate internal photoelectric effects, showing enhanced current responses under UV illumination. Thermal analysis reveals distinct decomposition profiles, highlighting the superior thermal stability of PVI_m. Overall, PVI_m-based materials possess potential applications in optoelectronics, sensing, and other fields requiring tunable conductive polymers.

REFERENCES

1. Hall N. Twenty-five years of conducting polymers // Chem. Commun. – 2003. – No. 1. – P.1-4.
2. Huang W.S., Humphrey B.D., MacDiarmid A.G. Polyaniline, a novel conducting polymer. Morphology and chemistry of its oxidation and reduction in aqueous electrolytes // J. Chem. Soc. Faraday Trans. 1. – 1986. – Vol.82. – P.2385-2400.
3. Design, synthesis, and control of conducting polymer architectures: structurally homogeneous poly(3alkylthiophenes) / McCullough R.D., Lowe R.D., Jayaraman M., Anderson D.L. // J. Org. Chem. – 1993. – Vol.58. – P.904-912.
4. Wang J., Dai J., Yarlagadda T. Carbon nanotube-conducting-polymer composite nanowires // Langmuir. – 2005. – Vol.21. – P.9-12.
5. Organic electronics: graphene-conducting polymer hybrid transparent electrodes for efficient organic optoelectronic devices / Lee B.H., Lee J.H., Kahng Y.H., Kim N., Kim Y.J., Lee J., et al. // Adv. Funct. Mater. – 2014. – Vol.24. – P.1960.
6. Microstructure, residual stress, and intermolecular force distribution maps of graphene/polymer hybrid composites: nanoscale morphology-promoted synergistic effects / Gupta S., McDonald B., Carrizosa S.B., Price C. // Compos. B Eng. – 2016. – Vol.92. – P.175-192.
7. Gupta S., Price C., Heintzman E. Conducting polymer nanostructures and nanocomposites with carbon nanotubes: hierarchical assembly by molecular electrochemistry, growth aspects and property characterization // J. Nanosci. Nanotechnol. – 2016. – Vol.16. – P.374-391.
8. Cantwell W.J., Morton J. The impact resistance of composite materials – a review // Composites. – 1991. – Vol.22. – P.347-362.
9. The specific effect of graphene additives in polyaniline-based nanocomposite layers on performance characteristics of electroluminescent and photovoltaic devices / Gribkova O.L., Omelchenko O.D., Tameev A.R., Lypenko D.A., Nekrasov A.A.,

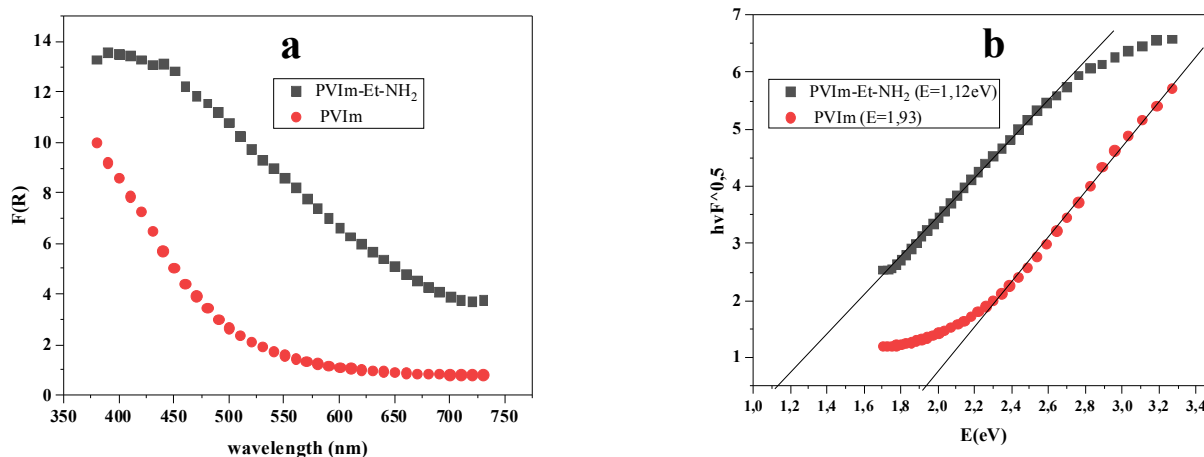


Fig. 8. Band gaps of PVI_m and PVI_m-Et-NH₂ materials

Posudievskii O.Y., et al. // *High Energy Chem.* – 2016. – Vol.50. – P.134-138.

10. *A new synthetic route to enhance polyaniline assembly on carbon nanotubes in tubular composites* / Biju P., Jining X., Jose K.A., Vijay K.V. // *Smart Mater. Struct.* – 2004. – Vol.13. – Art. No. N105.

11. *Kuo C.T., Chiou W.H.* Field-effect transistor with polyaniline thin film as semiconductor // *Synth. Met.* – 1997. – Vol.88. – P.23-30.

12. *Conducting polymer transistors making use of activated carbon gate electrodes* / Tang H., Kumar P., Zhang S., Yi Z., de Crescenzo G., Santato C., et al. // *ACS Appl. Mater. Interfaces.* – 2015. – Vol.7. – P.969-973.

13. *Polyaniline electrochromic devices with transparent graphene electrodes* / Zhao L., Zhao L., Xu Y., Qiu T., Zhi L., Shi G. // *Electrochim. Acta.* – 2009. – Vol.55. – P.491-497.

14. *A complementary electrochromic device based on carbon nanotubes/conducting polymers* / Shen K.Y., Hu C.W., Chang L.C., Ho K.C. // *Sol. Energy Mater. Sol. Cells.* – 2012. – Vol.98. – P.294-299.

15. *The effect of carbon nanofillers on the performance of electromechanical polyaniline-based composite actuators* / Garcia-Gallegos J.C., Martin-Gullon I., Conesa J.A., Vega-Cantu Y.I., Rodriguez-Macias F.J. // *Nanotechnology.* – 2016. – Vol.27. – Art. No. 015501.

Received 16.02.2025

СИНТЕЗ, ЕЛЕКТРОФІЗИЧНІ ТА ОПТИЧНІ ВЛАСТИВОСТІ ПРОВІДНИХ ПОЛІМЕРІВ НА ОСНОВІ ПОЛІ(1-N-ВІНІЛІМІДАЗОЛУ)

Сардорбек Отажонов, Хамдам Акбаров, Нуритдин Каттаев, Ельюр Бердимуродов, Абдугафур Мамадалімов, Шохзод Норбеков, Йон Іл-Лі

Полі(1-N-вінілімідазол) (PVI_m) було одержано радикальною полімеризацією 1-N-вінілімідазолу в бензольному розчині під інертною атмосферою за температури 60°C. Гідрофільний похідний полімер було синтезовано хімічною модифікацією PVI_m 3-бромопропіламіном гідробромідом. Структуру синтезованих полімерів досліджено методом ІЧ спектроскопії. Вивчали електрофізичні та оптичні властивості PVI_m і його похідних. Визначено температурну залежність електропровідності, вольтамперометричну поведінку, кінетику фотопровідності та значення оптичної забороненої зони цих полімерних матеріалів. Дослідження здійснювались в температурному діапазоні 300–360 K і при напрузі 0–100 V. Показано, що електропровідність у всіх зразках підпорядковується закону Ома.

Ключові слова: 1-N-вінілімідазол; радикальна полімеризація; хімічна модифікація; електропровідність; фотопровідність; вольтамперометричні характеристики.

SYNTHESIS, ELECTROPHYSICAL, AND OPTICAL PROPERTIES OF CONDUCTIVE POLYMERS BASED ON POLY(1-N-VINYLMIDAZOLE)

Sardorbek Otajonov^a, Khamdam Akbarov^{a,}, Nuritdin Kattaev^a, Elyor Berdimurodov^a, Abdugafur Mamadalimov^b, Shokhzod Norbekov^b, Yong Il-Lee^c*

^a Department of Chemistry, National University of Uzbekistan, Tashkent, Uzbekistan

^b Department of Physics, National University of Uzbekistan, Tashkent, Uzbekistan

^c Department of Chemistry, Changwon National University, Changwon, Republic of Korea

* e-mail: akbarov_Kh@rambler.ru

Poly(1-N-vinylimidazole) (PVI_m) was obtained by the radical polymerization of 1-N-vinylimidazole in a benzene solution under an inert atmosphere at a temperature of 60°C. Its hydrophilic derivative was synthesized by chemical modification of PVI_m with 3-bromopropylamine hydrobromide. The structure of the synthesized polymers was studied by IR spectroscopy. The electrophysical and optical properties of PVI_m and its derivatives were studied. The temperature dependence of electrical conductivity, voltammetric behavior, photoconductivity kinetics, and optical band gap values of these polymer materials were determined. This work was carried out in the 300–360 K temperature range and in the 0–100 V voltage range. It was confirmed that electrical conductivity in all samples obeyed Ohm's law.

Keywords: 1-N-vinylimidazole; radical polymerization; chemical modification; electrical conductivity; photoconductivity; voltammetric characteristics.

REFERENCES

- Hall N. Twenty-five years of conducting polymers. *Chem Commun.* 2003; (1): 1-4. doi: 10.1039/B210718J.
- Huang WS, Humphrey BD, MacDiarmid AG. Polyaniline, a novel conducting polymer. Morphology and chemistry of its oxidation and reduction in aqueous electrolytes. *J Chem Soc Faraday Trans 1.* 1986; 82: 2385-2400. doi: 10.1039/F19868202385.
- McCullough RD, Lowe RD, Jayaraman M, Anderson DL. Design, synthesis, and control of conducting polymer architectures: structurally homogeneous poly(3alkylthiophenes). *J Org Chem.* 1993; 58: 904-912. doi: 10.1021/jo00056a024.
- Wang J, Dai J, Yarlagadda T. Carbon nanotube–conducting-polymer composite nanowires. *Langmuir.* 2005; 21: 9-12. doi: 10.1021/la0475977.
- Lee BH, Lee JH, Kahng YH, Kim N, Kim YJ, Lee J, et al. Organic electronics: graphene-conducting polymer hybrid transparent electrodes for efficient organic optoelectronic devices. *Adv Funct Mater.* 2014; 24: 1960. doi: 10.1002/adfm.201470086.
- Gupta S, McDonald B, Carrizosa SB, Price C. Microstructure, residual stress, and intermolecular force distribution maps of graphene/polymer hybrid composites: nanoscale morphology-promoted synergistic effects. *Compos B Eng.* 2016; 92: 175-192. doi: 10.1016/j.compositesb.2016.02.049.

7. Gupta S, Price C, Heintzman E. Conducting polymer nanostructures and nanocomposites with carbon nanotubes: hierarchical assembly by molecular electrochemistry, growth aspects and property characterization. *J Nanosci Nanotechnol*. 2016; 16: 374-391. doi: 10.1166/jnn.2016.10721.

8. Cantwell WJ, Morton J. The impact resistance of composite materials – a review. *Composites*. 1991; 22: 347-362. doi: 10.1016/0010-4361(91)90549-V.

9. Gribkova OL, Omelchenko OD, Tameev AR, Lypenko DA, Nekrasov AA, Posudievskii OY, et al. The specific effect of graphene additives in polyaniline-based nanocomposite layers on performance characteristics of electroluminescent and photovoltaic devices. *High Energy Chem*. 2016; 50: 134-138. doi: 10.1134/S001814391602003X.

10. Biju P, Jining X, Jose KA, Vijay KV. A new synthetic route to enhance polyaniline assembly on carbon nanotubes in tubular composites. *Smart Mater Struct*. 2004; 13: N105. doi: 10.1088/0964-1726/13/6/N02.

11. Kuo CT, Chiou WH. Field-effect transistor with polyaniline thin film as semiconductor. *Synth Met*. 1997; 88: 23-30. doi: 10.1016/S0379-6779(97)80879-X.

12. Tang H, Kumar P, Zhang S, Yi Z, de Crescenzo G, Santato C, et al. Conducting polymer transistors making use of activated carbon gate electrodes. *ACS Appl Mater Interfaces*. 2015; 7: 969-973. doi: 10.1021/am507708c.

13. Zhao L, Zhao L, Xu Y, Qiu T, Zhi L, Shi G. Polyaniline electrochromic devices with transparent graphene electrodes. *Electrochim Acta*. 2009; 55: 491-497. doi: 10.1016/j.electacta.2009.08.063.

14. Shen KY, Hu CW, Chang LC, Ho KC. A complementary electrochromic device based on carbon nanotubes/conducting polymers. *Sol Energy Mater Sol Cells*. 2012; 98: 294-299. doi: 10.1016/j.solmat.2011.11.020.

15. Garcia-Gallegos JC, Martin-Gullon I, Conesa JA, Vega-Cantu YI, Rodriguez-Macias FJ. The effect of carbon nanofillers on the performance of electromechanical polyaniline-based composite actuators. *Nanotechnology*. 2016; 27: 015501. doi: 10.1088/0957-4484/27/1/015501.